

Electronic Supplementary Information

**Porphyrin(2.1.2.1) as a Novel Binucleating Ligand: Synthesis and
Molecular Structures of Mono- and Di-rhodium(I) Complexes**

Songlin Xue,^{*a,b} Ningchao Liu,^a Peifeng Mei,^c Daiki Kuzuhara,^d Mingbo Zhou,^b Jianming Pan,^a Hiroko Yamada,^c and Fengxian Qiu^{*a}

^aSchool of Chemistry and Chemical Engineering, Jiangsu University, Zhenjiang 212013, China

^bKey Laboratory of the Assembly and Application of Organic Functional Molecules of Hunan Province, Changsha, Hunan 410081, China.

^cDivision of Materials Science, Nara Institute of Science and Technology (NAIST), 8916-5 Takayama-cho, Ikoma, Nara 630-0192, Japan

^dFaculty of Science and Engineering, Iwate University, 4-3-5 Ueda, Morioka 020-8551, Japan

E-mail: slxue@ujs.edu.cn
fxqiu@ujs.edu.cn

Contents

- 1. Instrument and Materials**
- 2. X-ray Analysis**
- 3. Theoretical Calculations**
- 4. Synthesis of 1Rh and 2Rh**
- 5. Supporting Figures**
- 6. Crystal Data**
- 7. References**

1. Instrument and Materials.

The UV-Vis absorption spectra were measured with a JASCO UV/VIS/NIR Spectrophotometer V-670. ^1H NMR spectra were recorded on a JNM-ECX 400 spectrometer using the residual solvent as the internal reference for ^1H ($\delta = 6.00$ ppm in $\text{C}_2\text{D}_2\text{Cl}_4$). APCI-FT-MS mass spectrum was recorded on a ThermoFisher Scientific spectrometer. Infrared spectra were measured on KBr pellets using a FT-IR (Thermo Nicolet, NEXUS, TM) spectrometer. The cyclic voltammetry were conducted in a solution of 0.1 M TBAP₆ in dry- CH_2Cl_2 with a scan rate of 0.1 V s^{-1} in an argon-filled cell. A glassy carbon electrode and a platinum wire were used as a working and a counter electrode, respectively. A saturated Calomel electrode (SCE) was used as reference electrodes. All solvents and chemicals were reagent grade quality, obtained commercially and used without further purification except as noted.

2. X-ray Analysis. X-ray crystallographic data for **1Rh** (CCDC: 2103006) and **2Rh** (CCDC: 2097323) complexes were recorded at 297 K and 193 K on a Rigaku R-Axis RAPID/S using Mo-K α radiation from the corresponding set of confocal optics. The structures were solved by direct methods and refined on F^2 by full-matrix least-squares using the CrystalClear and SHELXS-2000 program.¹

3. Theoretical Calculations. All density functional theory calculations were achieved with the Gaussian 09 program package.² The geometry of **1Rh** and **2Rh** was optimized at the Becke's three-parameter hybrid functional combined with the Lee-Yang-Parr correlation functional abbreviated as the B3LYP level of density functional theory with the 6-31G(d)/SDD level.

4. Synthesis of 1Rh and 2Rh

Porphyrin(2.1.2.1) **Por** was prepared according to our previous method.³

1Rh. Por (18 mg, 0.03 mmol) and NaOAc (12 mg, 0.15 mmol) were dissolved in 20 mL dry-CH₂Cl₂ at 0°C under nitrogen, then [Rh(CO)₂Cl]₂ (7 mg, 0.018 mmol) in 20 mL dry CH₂Cl₂ was dropped into mixture in 1 hour. The reaction mixture was stirred for extra 2 hours at 0°C. After removal of the solvent, the crude product was purified by silica gel column chromatography (*n*-hexane/CH₂Cl₂ = 1/3) to give **1Rh** in 55% (12 mg, 0.0165 mmol) as a brown-red solid, **2Rh** was obtained as by-product in 5 % (1.4 mg, 0.0015 mmol). ¹H NMR (400 MHz, C₂D₂Cl₄, 298 K) δ = 11.96 (brs, 1H, NH), 7.57-7.51 (m, 8H, phenyl), 7.47-7.36 (m, 8H, phenyl), 7.36-7.32 (m, 2H, phenyl), 6.54 (d, *J* = 4 Hz, 1H, pyrrole), 6.50 (d, *J* = 4 Hz, 2H, pyrrole), 6.47 (d, *J* = 4 Hz, 1H, pyrrole), 6.40 (d, *J* = 4 Hz, 2H, pyrrole), 6.32 (d, *J* = 4 Hz, 1H, pyrrole), 6.26 (d, *J* = 4 Hz, 1H, pyrrole) ppm. APCI-FT-MS: Calcd. for C₄₄H₂₇N₄O₂Rh = 746.1189 [M]⁺, Found: 747.12097 [M+H]⁺. UV-vis-NIR (in CH₂Cl₂) λ [nm] (ϵ [M⁻¹ cm⁻¹]): 434 (73100), 456 (78100), 497 (35800), 545 (21100). IR (KBr): $\nu_{C=O}$ = 2064, 1996 cm⁻¹.

2Rh. Condition a: **Por** (17.6 mg, 0.03 mmol), [Rh(CO)₂Cl]₂ (58.5 mg, 0.15 mmol) and NaOAc (12 mg, 0.15 mmol) were dissolved in 20 mL dry-CH₂Cl₂ at 45°C for 12 hours under nitrogen. After removal of the solvent, the crude product was purified by silica gel column chromatography (*n*-hexane/CH₂Cl₂ = 2/1) to give **2Rh** in 90% (24 mg, 0.027 mmol) as a brown-red solid. **Condition b:** **Por** (17.6 mg, 0.03 mmol), [Rh(CO)₂Cl]₂ (58.5 mg, 0.15 mmol) and NaOAc (12 mg, 0.15 mmol) were dissolved in 10 mL dry-toluene at 100°C for 12 hours under nitrogen. After removal of the solvent, the crude product was purified by silica gel column chromatography (*n*-hexane/CH₂Cl₂ = 2/1) to give **2Rh** in 85% (23 mg, 0.026 mmol) as brown-red solid. ¹H NMR (400 MHz, C₂D₂Cl₄, 298 K) δ = 7.64-7.62 (m, 4H, phenyl), 7.49-7.47 (m, 4H, phenyl), 7.43-7.39 (m, 8H, phenyl), 7.20 (brs, 2H, phenyl), 6.32 (d, *J* = 4 Hz, 4H, pyrrole), 6.04 (d, *J* = 4 Hz, 4H, pyrrole) ppm. APCI-FT-MS: Calcd. for C₄₆H₂₆N₄O₄Rh₂ = 904.0064 [M]⁺, Found: 905.01025 [M+H]⁺. UV-vis-NIR (in CH₂Cl₂) λ [nm] (ϵ [M⁻¹ cm⁻¹]): 333 (28100), 393 (23300), 496 (106000). IR (KBr): $\nu_{C=O}$ = 2071, 2002 cm⁻¹.

5. Supporting Figures

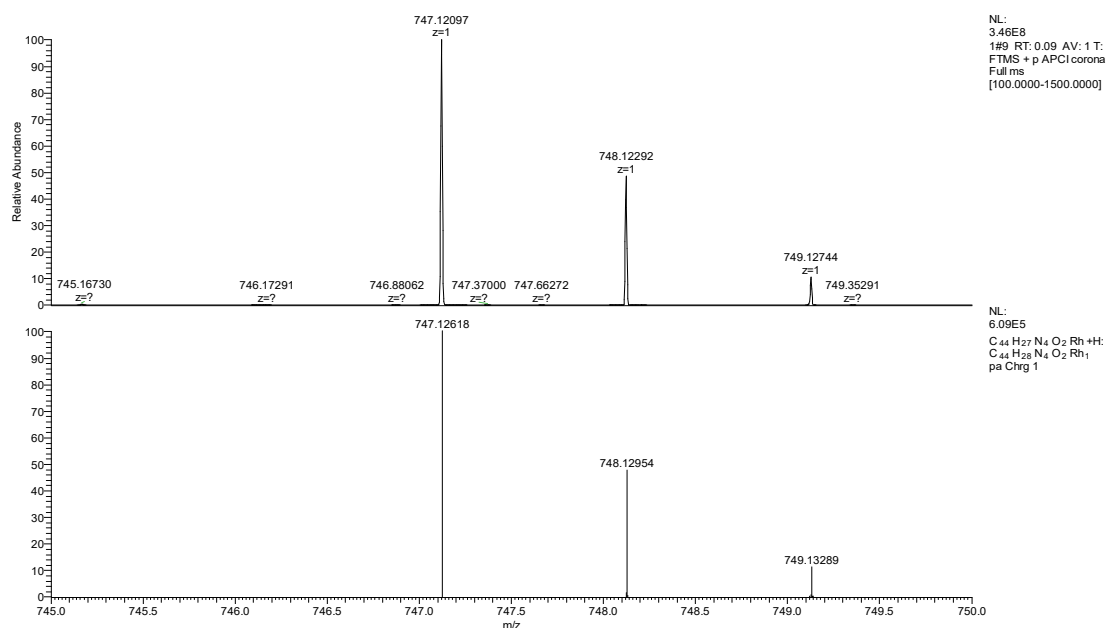


Fig. S1 Observed (top) and simulated (bottom) APCI-FT-MS spectrum of **1Rh**.

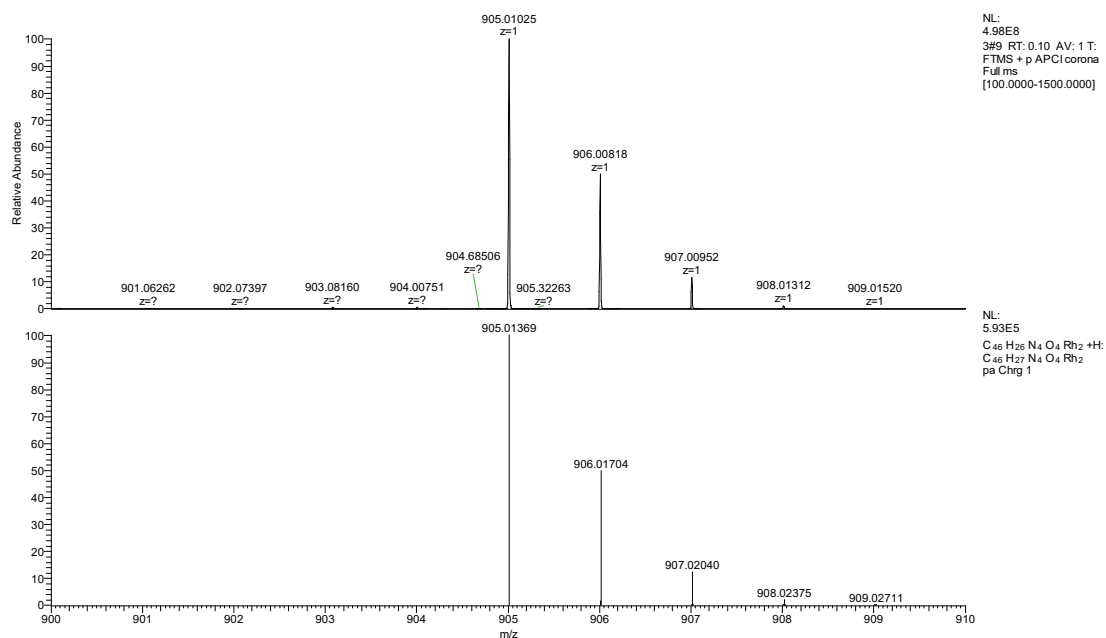


Fig. S2 Observed (top) and simulated (bottom) APCI-FT-MS spectrum of **2Rh**.

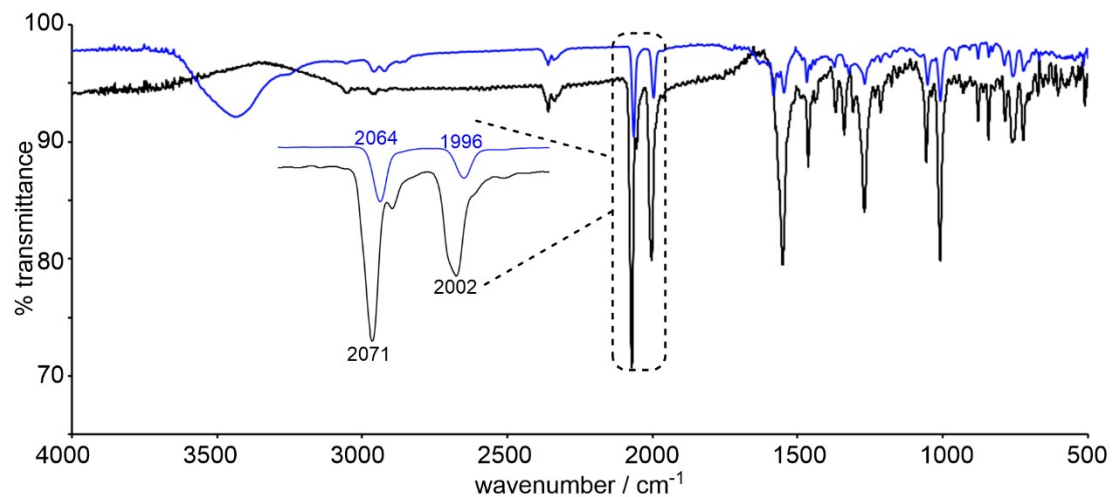


Fig. S3 IR spectra of **1Rh** (blue line) and **2Rh** (black line).

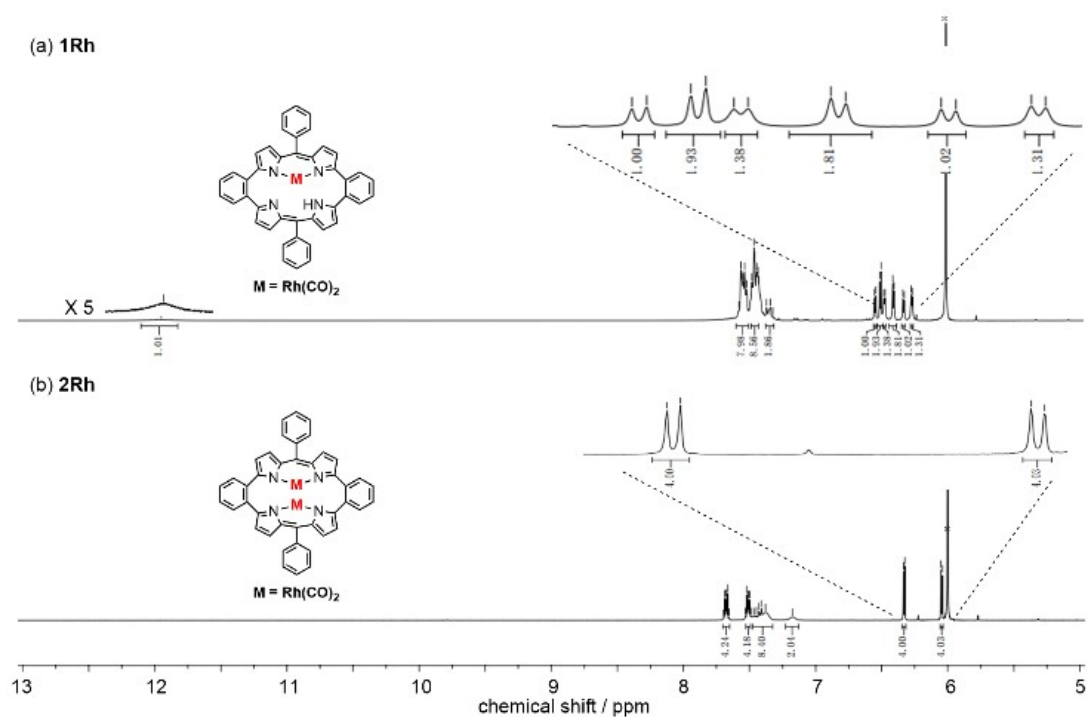


Fig. S4 ^1H NMR spectra of (a) **1Rh** and (b) **2Rh** in $\text{C}_2\text{D}_2\text{Cl}_4$ at 293 K. The asterisks indicate residual solvent peaks.

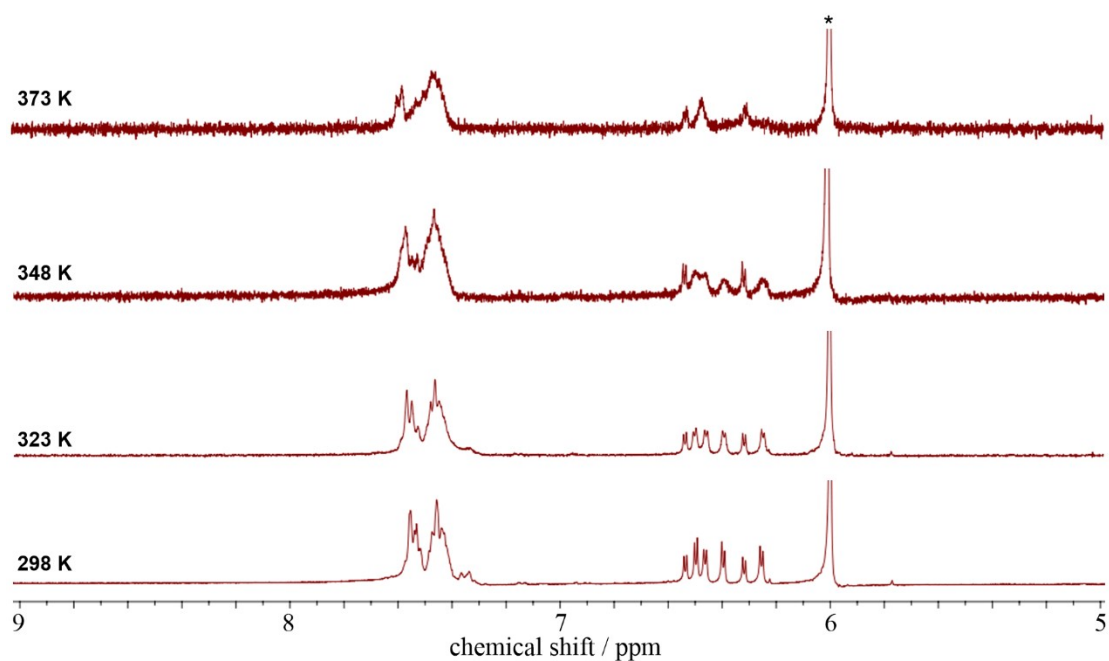


Fig. S5 Variable temperature ^1H NMR spectra of **1Rh** in $\text{C}_2\text{D}_2\text{Cl}_4$. The asterisks indicate residual solvent peaks.

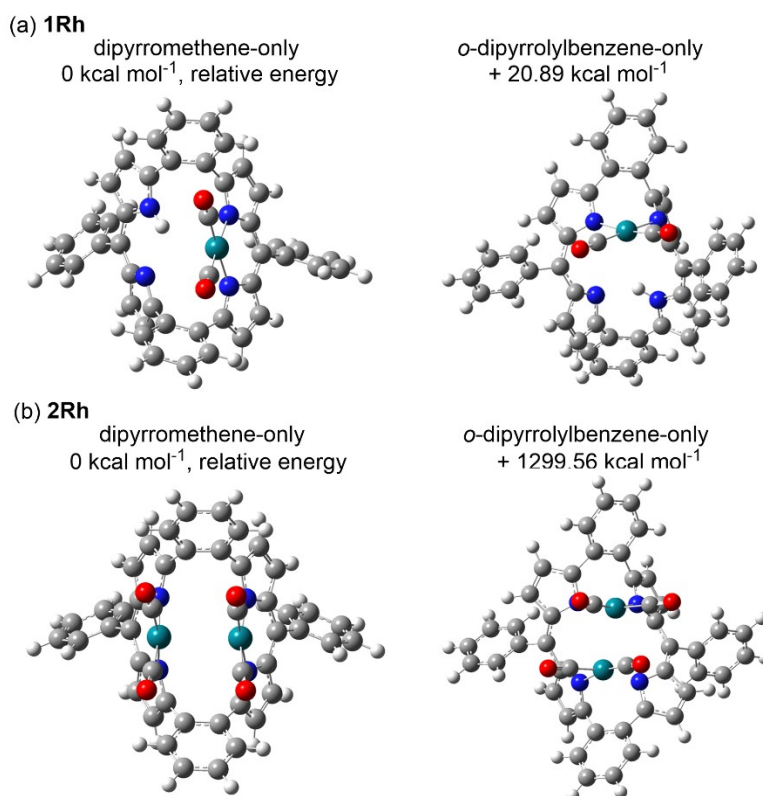


Fig. S6 Optimized structures and relative energies of (a) **1Rh** and (b) **2Rh** for dipyrromethene-only (0 kcal mol⁻¹, relative energy), and *o*-dipyrrolylbenzene-only coordination modes.

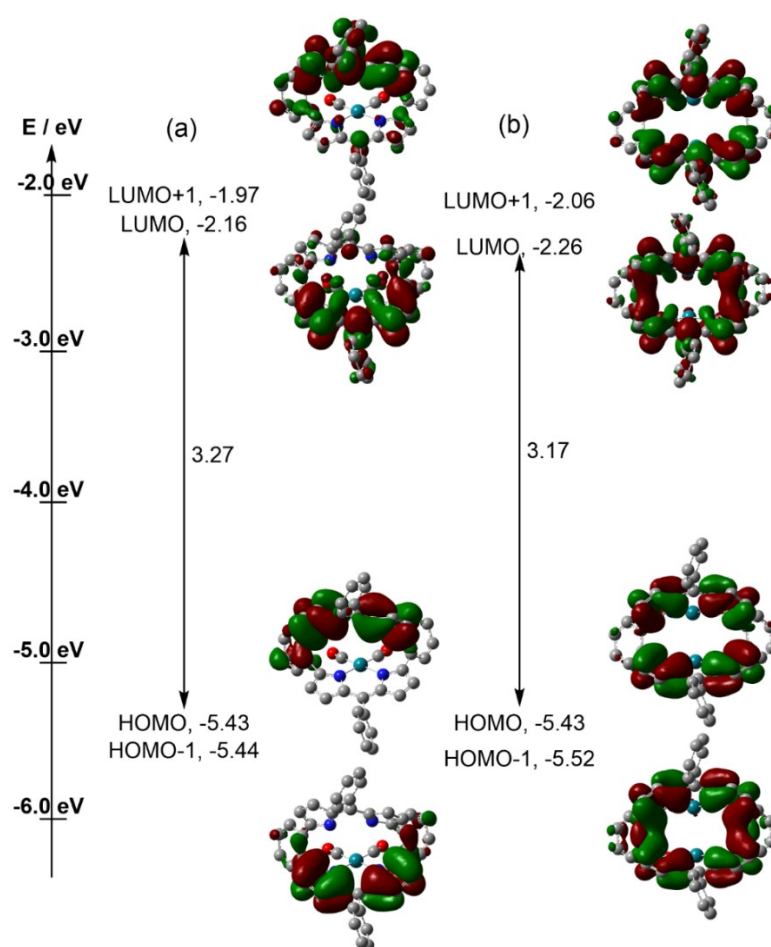


Fig. S7 Frontier molecular orbitals and energy diagrams of (a) **1Rh** and (b) **2Rh** calculated at the B3LYP/6-31G(d)/SDD level of theory.

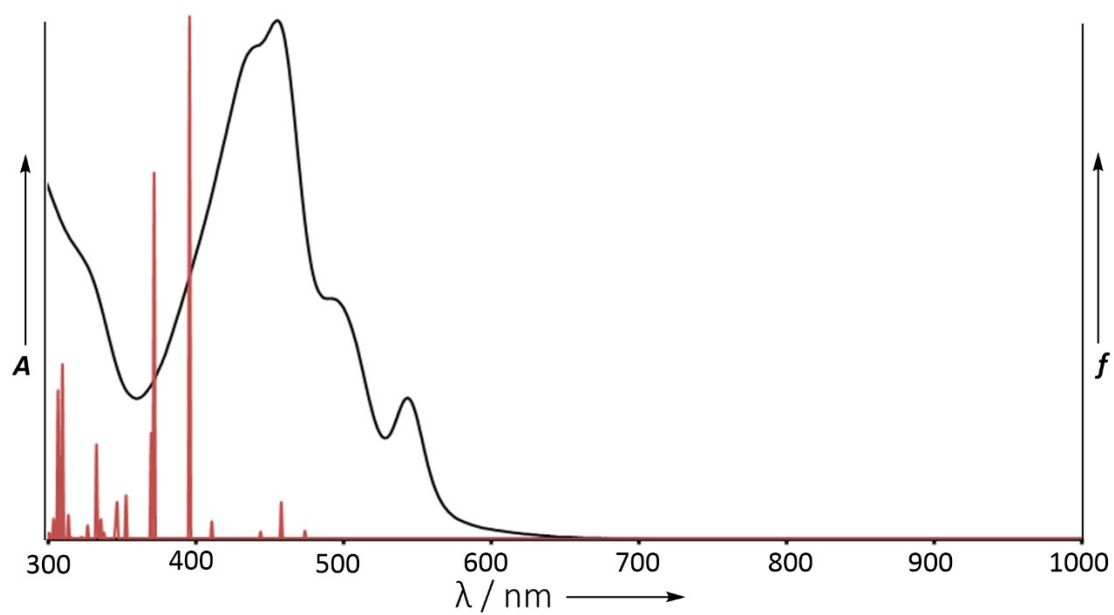


Fig. S8 The UV-Vis absorption spectrum (black line, left axis) and oscillator strengths (red bar, right axis), which is calculated at the B3LYP/6-31G(d)/SDD level of theory of **1Rh**.

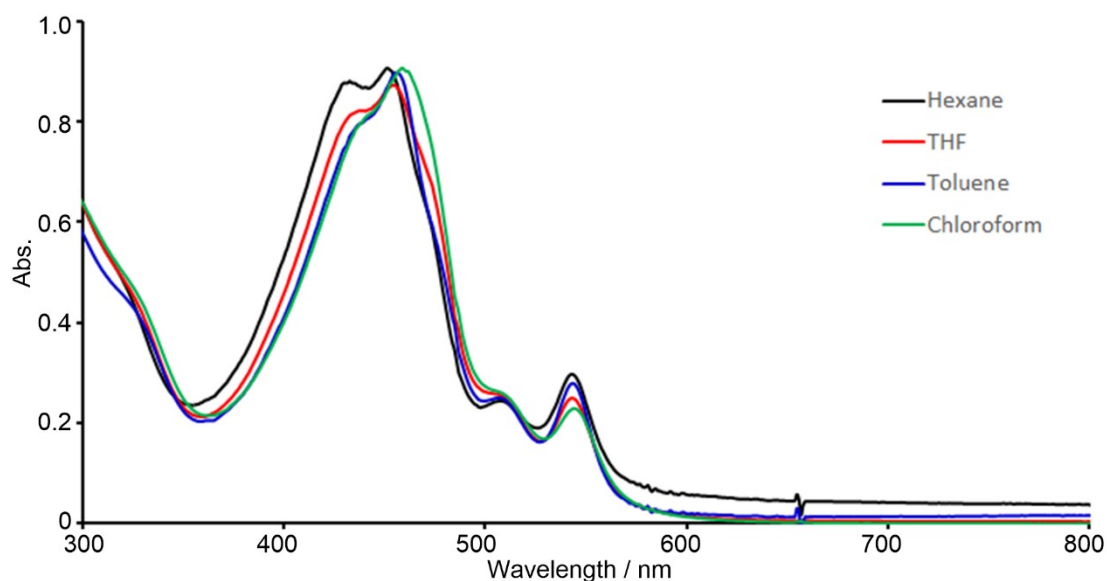


Fig. S9 UV-Vis absorption spectra of **1Rh** in hexane (black line), toluene (blue line), chloroform (green line) and THF (red line).

Table S1. Major composition, vertical excitation energies (E , eV/nm) and oscillator strengths (f) for the lowest optically allowed excited states of **1Rh**, calculated at the B3LYP/6-31G(d)/SDD level of theory.

State	Composition	Exci.	f
1	H* -> L	2.61/474	0.0063
2	H-1 -> L (0.58416) H -> L+1 (0.33884)	2.71/458	0.0278

*H = HOMO, Highest Occupied Molecular Orbital, L = LUMO, Lowest Unoccupied Molecular Orbital.

6. Crystal Data

Table S2. Crystal data of **1Rh**

Empirical formula	$C_{44}H_{27}N_4O_2Rh$
Formula weight	746.60
Temperature	193.0 K
Wavelength	1.34139 Å
Crystal system	Orthorhombic
Space group	$Pna2_1$
Unit cell dimensions	$a = 22.1380(15)$ Å $\alpha = 90^\circ$ $b = 6.6176(4)$ Å $\beta = 90^\circ$ $c = 22.4596(11)$ Å $\gamma = 90^\circ$
Volume	$3290.3(3)$ Å ³
Z	4
Density (calculated)	1.507 Mg/m ³
Absorption coefficient	3.037 mm ⁻¹
$F(000)$	1520
Crystal size	$0.08 \times 0.06 \times 0.05$ mm ³
Theta range for data collection	3.474 to 55.295° .
Index ranges	$-26 \leq h \leq 26$, $-8 \leq k \leq 8$, $-27 \leq l \leq 21$
Reflections collected	31791
Independent reflections	5774 [$R(\text{int}) = 0.1693$]
Completeness to theta = 53.594°	99.2 %
Absorption correction	Semi-empirical from equivalents
Max. and min. transmission	0.7508 and 0.5473
Refinement method	Full-matrix least-squares on F^2
Data / restraints / parameters	5774 / 50 / 465
Goodness-of-fit on F^2	1.014
Final R indices [$I > 2\sigma(I)$]	$R_1 = 0.0977$, $wR_2 = 0.2401$
R indices (all data)	$R_1 = 0.1693$, $wR_2 = 0.2850$
Absolute structure parameter	0.24(4)
Extinction coefficient	n/a
Largest diff. peak and hole	1.877 and -0.687 e.Å ⁻³

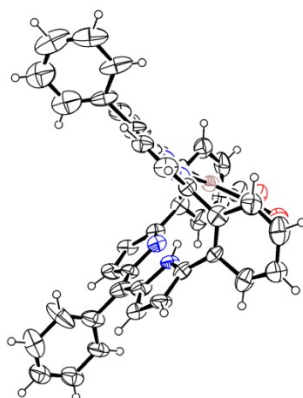
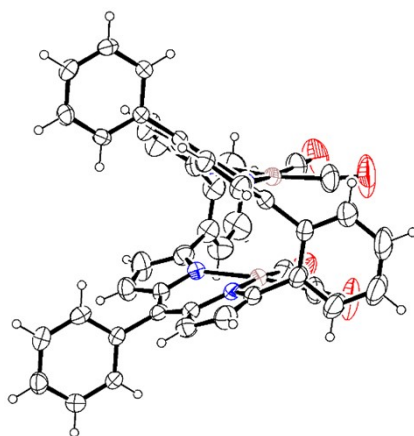


Fig.S10 Crystal structure of **1Rh**. The thermal ellipsoids represent for 40% probability.

Table S3. Crystal data of **2Rh**

Empirical formula	$\text{C}_{46}\text{H}_{26}\text{N}_4\text{O}_4\text{Rh}_2$	
Formula weight	904.53	
Temperature	296.15 K	
Wavelength	0.71073 Å	
Crystal system	Triclinic	
Space group	$P\bar{1}$	
Unit cell dimensions	$a = 13.6924(12)$ Å	$\alpha = 90.341(2)^\circ$
	$b = 18.0240(17)$ Å	$\beta = 104.620(2)^\circ$
	$c = 26.204(2)$ Å	$\gamma = 98.347(2)^\circ$
Volume	6185.2(10) Å ³	
Z	6	
Density (calculated)	1.457 Mg/m ³	
Absorption coefficient	0.847 mm ⁻¹	
$F(000)$	2712	
Crystal size	0.09 x 0.08 x 0.01 mm ³	
Theta range for data collection	1.555 to 28.130°.	
Index ranges	$-18 \leq h \leq 18, -22 \leq k \leq 23, -34 \leq l \leq 31$	
Reflections collected	53450	
Independent reflections	30021 [$R(\text{int}) = 0.0415$]	
Completeness to $\theta = 25.242^\circ$	99.9 %	
Absorption correction	Semi-empirical from equivalents	
Max. and min. transmission	0.7457 and 0.6354	
Refinement method	Full-matrix least-squares on F^2	
Data / restraints / parameters	30021 / 0 / 1513	
Goodness-of-fit on F^2	0.917	
Final R indices [$I > 2\sigma(I)$]	$R_1 = 0.0495, wR_2 = 0.1034$	
R indices (all data)	$R_1 = 0.1087, wR_2 = 0.1266$	
Extinction coefficient	n/a	
Largest diff. peak and hole	0.846 and -0.787 e.Å ⁻³	

**Fig. S11** Crystal structure of **2Rh**. The thermal ellipsoids represent for 40% probability.

7. References

- (1) G. Sheldrick, *Acta Cryst.* **2008**, *A64*, 112.
- (2) Gaussian 09, Revision B.01, M. J. Frisch, G. W. Trucks, H. B. Schlegel, G. E. Scuseria, M. A. Robb, J. R. Cheeseman, G. Scalmani, V. Barone, B. Mennucci, G. A. Petersson, H. Nakatsuji, M. Caricato, X. Li, H. P. Hratchian, A. F. Izmaylov, J. Bloino, G. Zheng, J. L. Sonnenberg, M. Hada, M. Ehara, K. Toyota, R. Fukuda, J. Hasegawa, M. Ishida, T. Nakajima, Y. Honda, O. Kitao, H. Nakai, T. Vreven, J. A. Montgomery, Jr., J. E. Peralta, F. Ogliaro, M. Bearpark, J. J. Heyd, E. Brothers, K. N. Kudin, V. N. Staroverov, T. Keith, R. Kobayashi, J. Normand, K. Raghavachari, A. Rendell, J. C. Burant, S. S. Iyengar, J. Tomasi, M. Cossi, N. Rega, J. M. Millam, M. Klene, J. E. Knox, J. B. Cross, V. Bakken, C. Adamo, J. Jaramillo, R. Gomperts, R. E. Stratmann, O. Yazyev, A. J. Austin, R. Cammi, C. Pomelli, J. W. Ochterski, R. L. Martin, K. Morokuma, V. G. Zakrzewski, G. A. Voth, P. Salvador, J. J. Dannenberg, S. Dapprich, A. D. Daniels, O. Farkas, J. B. Foresman, J. V. Ortiz, J. Cioslowski, and D. J. Fox, Gaussian, Inc., Wallingford CT, 2010.
- (3) (a) S. Xue, D. Kuzuhara, N. Aratani, H. Yamada, *Org. Lett.* **2019**, *21*, 2069; (b) D. Kuzuhara, W. Furukawa, A. Kitashiro, N. Aratani, H. Yamada, *Chem. - Eur. J.* **2016**, *22*, 10671.